CHEMISTRY OF MATERIALS
Article

Chem. Mater. **2010,** *22,* 1149–1154 1149
DOI:10.1021/cm9024342

$Ag_3Fe(VO_4)_2$ and $AgFeV_2O_7$: Synthesis, Structure, and Electrochemical Characteristics of Two New Silver Iron(III) Vanadates†

Gregory A. Becht,‡ John T. Vaughey,§ and Shiou-Jyh Hwu*,‡

‡*Department of Chemistry, Clemson University, Clemson, South Carolina 29634-0973 and*
§*Chemical Sciences and Engineering, Argonne National Laboratory, Argonne, Illinois 60439-4837*

Received August 8, 2009. Revised Manuscript Received November 24, 2009

The structural features and electrochemical properties of two new silver iron(III) vanadates have been determined, and their relevance to cathode materials for primary lithium battery devices is reported. $Ag_3Fe(VO_4)_2$ (**SFVO-1**) and $AgFeV_2O_7$ (**SFVO-2**) were isolated via a pseudoternary ($Ag_2O-Fe_2O_3-V_2O_5$) system at 600 °C. The crystallographic data of the phases are the following: $Ag_3Fe(VO_4)_2$ monoclinic $C2/c$ (no. 15), a = 9.771(2) Å, b = 5.153(1) Å, c = 14.325(3) Å, β = 93.85(3)°, V = 719.7(2) Å^3, Z = 4; $AgFeV_2O_7$, triclinic, $P\bar{1}$ (no. 2), a = 5.603(1) Å, b = 7.485(2) Å, c = 7.644(2) Å, α = 65.07(3)°, β = 89.48(3)°, γ = 78.98(3)°, V = 284.4(1) Å^3, Z = 2. The single crystal X-ray diffraction studies show that the Ag^+ cations reside in the open space of layered (**SFVO-1**) and channeled (**SFVO-2**) Fe−O−V frameworks. The extended electrochemical capacity above 2 V (vs Li/Li^+) in these phases is consistent with their higher $(Ag^+ + Fe^{3+})/V^{5+}$ ratios, compared to the corresponding Ag^+/V^{5+} in $Ag_2V_4O_{11}$ (SVO). The discharge voltage of **SFVO-1** exhibits a short initial plateau at ∼3.15 V, corresponding to the reduction of 0.5 × [Ag(I) → Ag(0)], followed by an abrupt drop to ∼2.3−2.0 V where the remaining silver (2.5 equiv Li) and some of the framework iron (0.8 equiv Li) are reduced. **SFVO-2** has a nominal capacity of 293 mA h/g exhibiting several plateaulike features between 2.5 and 2.0 V. **SFVO-1,2** represents the first family of silver iron(III) vanadate phases that have been systematically investigated.

Introduction

Vanadium oxides constitute one of the earliest and most studied oxides as an electrode for lithium battery applications.[1] They have several advantages such as large capacity, high voltage, and excellent kinetics that make them attractive electrode materials. However, their tendency to become amorphous upon cycling limits their cycle lifetimes and commercial viability in electrochemical cells. To increase the stability of the framework during discharge, researchers have evaluated the effect of adding other metal cations to the structure, i.e., LiV_3O_8, $Ag_2V_4O_{11}$, or MnV_2O_5.[2] This approach has had some successes in stabilizing the framework during cycling by increasing the average coordination of the vanadium cation as well as adding a structural element that binds the various layers together.

Silver vanadium oxide, $Ag_2V_4O_{11}$ (SVO), has been known for its superior electrochemical properties in a primary lithium battery configuration and has been used extensively in implantable medical devices.[3] The layered-like structure of the V−O framework provides a pathway for the diffusion of silver and lithium ions creating a high electrochemical potential and power capability for the material. These characteristics combine to make it a good cathode material for high powered devices such as cardiac defibrillators. On discharge, SVO can insert up to ca. 7 mol of lithium per formula unit at an initial open circuit voltage of 3.25 V (vs Li) corresponding to the reduction of the two silver cations, Ag(I) → Ag(0).[4] Overall, the theoretical capacity of SVO is 315 mA h/g; however, < 15% (47 mA h/g) is above the 3 V.

Because the battery is used to rapidly charge the capacitors in the defibrillator, high power capability when the voltage is above 3 V is an important variable. For many years, a goal of this field of research has been to extend the capacity of the cathode above that voltage, while maintaining its stability and rate capability. In order to achieve this, Takeuchi et al. suggested that a greater Ag:V molar ratio is needed. However, the silver vanadates with Ag:V ratio greater than 1:2 tend to have very poor kinetics, low usable capacity, or low conductivity, such as those in $Ag_4V_2O_7$.[4]

An alternative approach to achieving a higher Ag:V ratio in a mixed metal oxide is to replace some of the

† Accepted as part of the 2010 "Materials Chemistry of Energy Conversion Special Issue".

(1) Whittingham, M. S. *Chem. Rev.* **2004**, *104*, 4271–4301.
(2) (a) Zhang, F.; Whittingham, M. S. *Electrochem. Commun.* **2000**, *2*, 69–71. (b) Selvaggi, A.; Croce, F.; Scrosati, B. *J. Power Sources* **1990**, *32*, 389–396. (c) Scrosati, B.; Selvaggi, A.; Croce, F.; Wang, G. *J. Power Sources* **1988**, *24*, 287–294. (d) Nassau, K.; Murphy, D. W. *J. Non-Cryst. Solids* **1981**, *44*, 297–304. (e) García-Alvarado, F.; Tarascon, J. M. *Solid State Ionics* **1994**, *73*, 247–254.
(3) (a) Crespi, A. M.; Somdahl, S. K.; Schmidt, C. L.; Skarstad, P. M. *J. Power Sources* **2001**, *96*, 33–38. (b) Schmidt, C. L.; Skarstad, P. M. *J. Power Sources* **2001**, *97−98*, 742–746. (c) Passerini, S.; Owens, B. B.; Coustier, F. *J. Power Souces* **2000**, *89*, 29–39.
(4) Takeuchi, K. J.; Marschilok, A. C.; Davis, S. M.; Leising, R. A.; Takeuchi, E. S. *Coord. Chem. Rev.* **2001**, *219−221*, 283–310.

Published on Web 12/21/2009

framework oxide anion with more electronegative fluoride anion. Recently, Poeppelmeier and co-workers have reported a new mixed-anion, oxide-fluoride phase, $Ag_4V_2O_6F_2$,[5] with a capacity above 3 V that is three times that of SVO (47 vs 148 mA h/g). In addition to the increased capacity, the addition of fluoride anion to the materials has increased the silver reduction potential to 3.52 V (270 mV higher than in SVO). This change is due to an inductive effect with incorporated fluoride now in the coordination sphere of the silver cation. However, there are two drawbacks for this material; the safety of preparation, due to the use of hydrofluoric acid,[6] and the lower intrinsic electronic conductivity of the material, which diminishes the power capability compared to SVO.[5]

In light of the studies in iron(III)-containing systems discussed in the previous reports[7] and the enhanced cell voltage due to induction effect of large oxyanions (polyanions) in transition metal phosphate compounds,[8] we have begun the search of new phase formation in the pseudoternary, $Ag_2O-Fe_2O_3-V_2O_5$, system. In these systems, fully oxidized vanadate anions may be employed as large polyanions. The idea to synthesize new silver-containing compounds with an extended capacity was to incorporate a second transition metal cation that provides a compatible reduction potential. Two new silver iron(III) vanadate phases, i.e., $Ag_3Fe(VO_4)_2$ (**SFVO-1**) and $AgFeV_2O_7$ (**SFVO-2**), were isolated via high-temperature, solid-state reactions. Herein, the synthesis, structure and electrochemical properties of silver vanadate based oxides incorporating multiple redox centers will be discussed for the first time. Both compounds show exceptional capacities because of the combined reduction of Ag^+/Ag^0 and Fe^{3+}/Fe^{2+}.

Experimental Section

Synthesis. Employing high-temperature, solid-state methods, sizable crystals of $Ag_3Fe(VO_4)_2$ (red) and $AgFeV_2O_7$ (black) were grown in the morphologies of plate and column, respectively. Single crystals were synthesized from the stoichiometric mixture of Ag_2O (1.5 mmol, Aesar, 99%), Fe_2O_3 (0.5 mmol, Aesar, 99.9%), and V_2O_5 (1.0 mmol, Aesar, 99.6%) for **SFVO-1** and Ag_2O (0.5 mmol, Aesar, 99%), Fe_2O_3 (0.5 mmol, Aesar, 99.9%), and V_2O_5 (1.0 mmol, Aesar, 99.6%) for **SFVO-2**. For both reactions, the reactants were ground together in an inert atmosphere drybox. The mixtures were loaded into a silica ampule and then sealed under vacuum. The reactions were heated to 600 °C at a rate of 1 °C/min, isothermed for 2 days, and finally cooled by 3 °C/min to room temperature.

Polycrystalline samples (see powder X-ray diffraction (PXRD) plots in Figures S1 and S2 and refined cell parameters in Tables S1 and S2 of the Supporting Information) were prepared in a gram size batch. Stoichiometric mixtures of reactants were ground together in air then loaded into an alumina crucible. The reactions were heated to 600 °C at a rate of 2 °C/min and held at that temperature for 2 days before being furnace cooled to room temperature. The samples were subject to regrind/reheat twice to increase the crystallinity and the yield of the product.

Table 1. Crystallographic Data for $Ag_3Fe(VO_4)_2$ and $AgFeV_2O_7$

empirical formula	$Ag_3Fe(VO_4)_2$	$AgFeV_2O_7$
FW	609.33	377.6
morphology, color	plate, red	column, black
crystal system	monoclinic	triclinic
crystal dimension, mm	0.24 × 0.39 × 0.26	0.14 × 0.19 × 0.16
space group, Z	$C2/c$ (no. 15), 4	$P\bar{1}$ (no. 2), 2
T, K	293(2)	293(2)
a, Å	9.771(2)	5.603(1)
b, Å	5.153(1)	7.485(2)
c, Å	14.325(3)	7.644(2)
α, deg		65.07(3)
β, deg	93.85(3)	89.48(3)
γ, deg		78.98(3)
V, Å^3	719.7(2)	284.4(1)
μ (Mo Kα), mm^{-1}	8.544	4.528
ρ_{calc}, g/cm^3	5.623	4.409
measured reflections	2629	2315
independent reflections	633	988
final $R1$, $wR2^a$ [$I > 2\sigma(I)$], GOF (all data)	0.0593/0.1249/1.068	0.0930/0.2836/1.139
secondary extinction coef	0.0109(8)	0.033(8)
largest diff peak/hole, e/Å^3	1.297/−2.007	4.614/−2.357

^{a} $R = \sum||F_o| - |F_c||/\sum|F_o|$; $wR2 = [\sum w(|F_o| - |F_c|)^2/\sum w|F_o|^2]^{1/2}$; $w = 1/[\sigma^2(F_o^2) + (0.0319P)^2 + 2.51P]$, where $P = (F_o^2 + 2F_c^2)/3$.

Crystallographic Studies. Red plate $Ag_3Fe(VO_4)_2$ and black column $AgFeV_2O_7$ crystals (see UV−vis plots in Figures S3 and S4, respectively) from different reactions were selected under an optical microscope equipped with a polarized light attachment and mounted on glass fibers for single-crystal X-ray diffraction study. The data collections were carried out at room temperature on a four-circle Rigaku AFC-8 diffractometer equipped with a charge-coupled device (CCD) area detector using graphite monochromated Mo Kα radiation (λ = 0.71073 Å). The structures were solved by direct methods with the SHELXTL-97 program and refined on F^2 by least-squares, full-matrix techniques.[9] Table 1 reports the crystallographic data of the structures, and Table 2 lists the atomic parameters. The large displacement parameters for Ag are quite unusual for it is the heaviest element in the structures. Low-temperature X-ray diffraction studies on multiple crystals grown under different reaction conditions were attempted to resolve this issue without any success. A long scan (increased scan time from the normal 5 to 40 s) was also employed, but it failed to resolve the issues associated with large displacement parameters. The larger than normal R value, especially for **SFVO-2**, is in part attributed to the small crystal size and poor crystal quality. Nonetheless, the accuracy of structural solution was established based on the success of stoichiometric yield synthesis of the title compounds (see Tables S1 and S2 and Figures S1 and S2).

Electrochemical Testing. Samples were ground and sieved to eliminate particles greater than 37 μm. The resulting powder was mixed into a slurry consisting of 80% active material, 10% poly(vinylidene difluoride) (PvDF) binder, and 10% acetylene black as conductive additive. The mixture was thoroughly

(5) Sorensen, E. M.; Izumi, H. K.; Vaughey, J. T.; Stern, C. L.; Poeppelmeier, K. R. *J. Am. Chem. Soc.* **2005**, *127*, 6347–6352.
(6) Segal, E. B. *Chem. Heal. Saf.* **2000**, *7*(1), 18–23.
(7) (a) Becht, G. A.; Vaughey, J. T.; Britt, R. L.; Eagle, C. T.; Hwu, S.-J. *Mater. Res. Bull.* **2008**, *43*, 3389–3396. (b) Becht, G.; Hwu, S.-J. *Chem. Mater.* **2006**, *18*, 4221–4223.
(8) (a) Padhi, A. K.; Nanjundaswamy, K. S.; Masquelier, C.; Okada, S.; Goodenough, J. B. *J. Electrochem. Soc.* **1997**, *144*(5), 1609–1613. (b) Goodenough, J. B. In *Lithium Ion Batteries*; Wakihara, M., Yamamoto, O., Eds.; Kodansha: Tokyo, 1998; Chapter I.
(9) (a) Sheldrick, G. M. In *Crystallographic Computing 3*; Sheldrick, G. M., Kruger, C., Goddard, R., Eds.; Oxford Univ. Press: London, 1985; pp 175−189. (b) Sheldrick, G. M. In *SHELXTL*, Version 6.10 Structure Determination Software Programs; Bruker Analytical Xray Systems Inc.: Madison, WI, 2001.

Table 2. Atomic Coordinates and Equivalent Displacement Parameters for $Ag_3Fe(VO_4)_2$ (SFVO-1) and $AgFeV_2O_7$ (SFVO-2)

$Ag_3Fe(VO_4)_2$ (**SFVO-1**)

atom	Wyckoff notation	*x*	*y*	*z*	U_{iso} (Å^2)[a]
Ag(1)	4*e*	0	0.0432(2)	3/4	0.045(1)
Ag(2)	8*f*	0.83891(9)	0.5575(2)	0.85980(6)	0.0303(7)
Fe	4*a*	0	0	1/2	0.011(1)
V	8*f*	0.6676(2)	1.0367(3)	0.8933(1)	0.010(1)
O(1)	8*f*	0.6669(8)	0.883(2)	0.7896(5)	0.035(5)
O(2)	8*f*	0.6076(6)	0.822(1)	0.9708(4)	0.014(3)
O(3)	8*f*	0.5607(7)	1.312(1)	0.8845(5)	0.020(4)
O(4)	8*f*	0.8358(7)	1.127(1)	0.9258(5)	0.011(3)

$AgFeV_2O_7$ (**SFVO-2**)

atom	Wyckoff notation	*x*	*y*	*z*	U_{iso} (Å^2)[a]
Ag	2*i*	0.1769(3)	0.3353(3)	0.9654(3)	0.022(1)
Fe	2*i*	−0.1729(5)	0.6791(4)	0.5241(4)	0.007(2)
V(1)	2*i*	0.3075(6)	0.7732(5)	0.2137(5)	0.007(2)
V(2)	2*i*	0.2950(6)	0.7843(5)	0.7449(5)	0.008(2)
O(1)	2*i*	0.099(3)	0.631(2)	0.362(2)	0.015(7)
O(2)	2*i*	0.073(3)	0.656(2)	0.724(2)	0.018(8)
O(3)	2*i*	0.223(3)	1.028(2)	0.593(2)	0.017(8)
O(4)	2*i*	0.326(3)	0.743(3)	0.990(2)	0.013(8)
O(5)	2*i*	0.564(3)	0.677(2)	0.700(2)	0.019(8)
O(6)	2*i*	0.590(3)	0.697(3)	0.326(2)	0.010(8)
O(7)	2*i*	0.212(3)	1.008(3)	0.165(2)	0.025(9)

[a] Equivalent isotropic *U* defined as one-third of the trace of the orthogonalized U_{ij} tensor.

mixed and laminated onto an Al-current collector and dried for 2 h to eliminate any residual solvent.

Electrochemical evaluation was done using Hohsun 2032 (1.6 cm^2) cell hardware. Half cells were built in an Ar-atmosphere glovebox using lithium metal as the counter electrode, 1.0 M $LiPF_6$ in EC/DEC (50/50), and Celgard 2325 separators. Cells were evaluated using a galvanostatic intermittent titration technique (GITT). Cells were discharged at a D/5 rate for 30 min followed by a 3 h equilibration down to 0.7 V.

Results

Crystal Structure. The X-ray single-crystal structure of $Ag_3Fe(VO_4)_2$ reveals a layered framework with respect to the Fe−O−V slabs. The Ag^+ cations reside in between the parallel slabs, as shown in Figure 1. Each slab consists of alternating FeO_6 octahedral and VO_4 tetrahedral units that share vertex oxygen atoms. The fourth oxygen atoms of the VO_4 units are pointing into the space between paralleled slabs.

The structure of $AgFeV_2O_7$ reveals a channeled framework where the Ag^+ cations reside. As shown in Figure 2, the channels are made of edges of Fe_2O_{10} dimers and pyrovanadate (V_2O_7) units. The dimers are made of two distorted FeO_6 octahedral units sharing *cis* edges. Four of the terminal oxygen atoms of the V_2O_7 unit are shared with four dimer units along [100] while the fifth oxygen is shared with another dimer to extend the lattice along the (011) plane in the three-dimensional structure.

$Ag_3Fe(VO_4)_2$ has two crystallographically independent Ag^+ cations that form largely distorted coordination geometries. As shown in Figure S5, the Ag^+ cations adopt two types of coordination geometry, one being tetrahedral ($Ag(1)O_4$) and the other trigonal bypyramidal ($Ag(2)O_5$). In $AgFeV_2O_7$, there is only one crystallographic Ag^+ cation that adopts distorted square pyramidal geometry.

Table 3. Bond Valence Sum of Cations in $Ag_3Fe(VO_4)_2$ and $AgFeV_2O_7$

$Ag_3Fe(VO_4)_2$		$AgFeV_2O_7$	
Ag(1)	0.95	Ag	0.92
Ag(2)	0.95	Fe	3.13
Fe	3.03	V(1)	5.04
V	5.04	V(2)	5.10

For $Ag_3Fe(VO_4)_2$, the Ag−O bond distances for the tetrahedral unit range from 2.324(5) to 2.433(6) Å, and for the trigonal bypyramidal, the range is 2.323(6)−2.533(6) Å. These distances are within good agreement of the sums of Shannon crystal radii: 2.35 Å (CN = 4) and 2.44 Å (CN = 5).[10] Therefore, the close to 1.0 bond valence sum (BVS) is expected (Table 3). However, for $AgFeV_2O_7$, the Ag−O bond distances have a much greater range, 2.25(5)−2.76(4) Å. The BVS calculation including all five of the bonds results in the BVS close to the expected value +1.0. If only the bonds that were within the range of the sum of Shannon crystal radii for 5-coordinate Ag^+ were used, i.e., Ag−O(2) 2.29(1) Å × 1 and Ag−O(7) 2.25(2) Å × 1, the BVS comes out with a much lower value, 0.63. Therefore, it was determined that the square pyramidal geometry was considered the coordination including one long Ag−O(2) 2.763, Ag−O(4) 2.728(5), and Ag−O(6) 2.647(5) Å. In any event, the silver forms a highly distorted square pyramidal geometry, with angles ranging from 63.6(5) to 117.3(5)°. The silver framework consists of edge-shared dimers, Ag_2O_8, which are expected to be the cause of the longer then normal Ag−O(2) distances.

Comparing the Ag^+ cation geometries between SFVOs and SVO, the former has a smaller Ag-coordination number (CN). In SVO, the coordination number of Ag^+ cations is 6. This gives the advantage of having a stronger induction effect on the Ag^+ cation with respect to high reduction voltage (3.25 V). In the **SFVO-1** and **SFVO-2** compounds discussed herein, the CNs are 4 and 5. Therefore, it is expected that the voltage could be slightly lower because of the lower induction effect.

The iron oxide coordination geometries in $Ag_3Fe(VO_4)_2$ and $AgFeV_2O_7$ form almost perfect octahedra with bonds ranging from 1.98(3) to 2.03(2) Å and 1.95(3) to 2.03(3) Å and angles 87.6(2)−92.4(2)° and 89.7(8)−92.7(7)°, respectively, comparable with the expected sum of Shannon crystal radii of a Fe−O bond 2.005 Å and the expected 90.0° angle for an octahedron. The vanadium geometries, although slightly distorted, are also in good agreement with the expected distances, i.e., 1.715 Å, and ∠V−O−V angles of a vanadium-centered VO_4 tetrahedron. In $Ag_3Fe(VO_4)_2$, the V−O distances range from 1.680(6) to 1.757(6) Å and ∠V−O−V angles from 106.3(3)

(10) Shannon, R. D. *Acta Crystallogr.* **1976**, *A32*, 751–767.

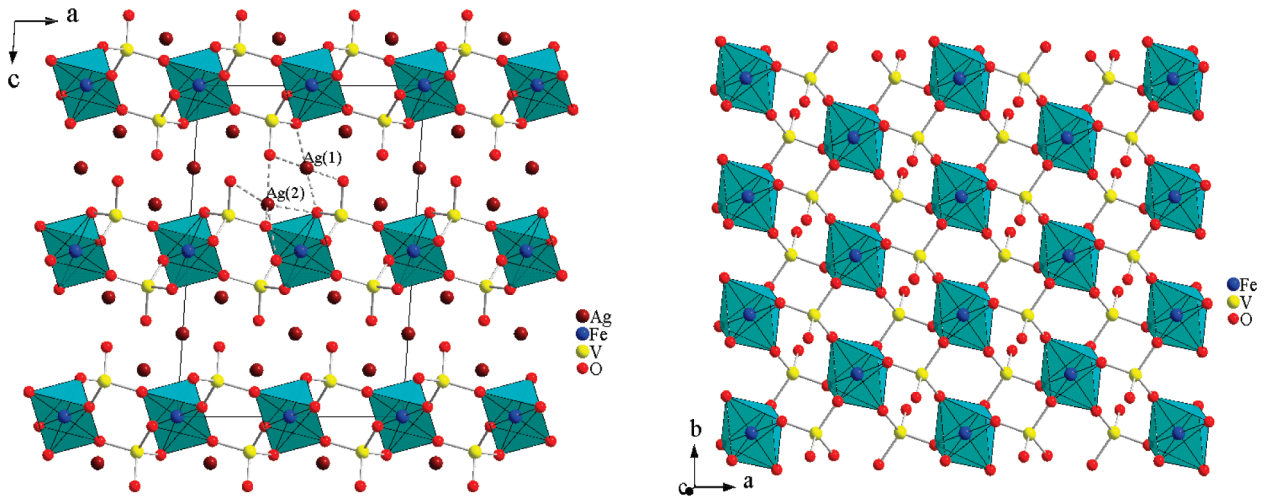

Figure 1. (left) Projected view of the $Ag_3Fe(VO_4)_2$ structure. The silver cations reside in the gap between the parallel sheets of alternating iron oxide octahedra (green) and vanadium oxide tetrahedral (balls and sticks). The selected Ag−O bonds are drawn for clarity. (right) Fe−O−V slab showing interconneted $[FeO_6]$ and $[VO_4]$ units. The unshared oxygen atoms of the $[VO_4]$ units point into the gap between parallel slabs.

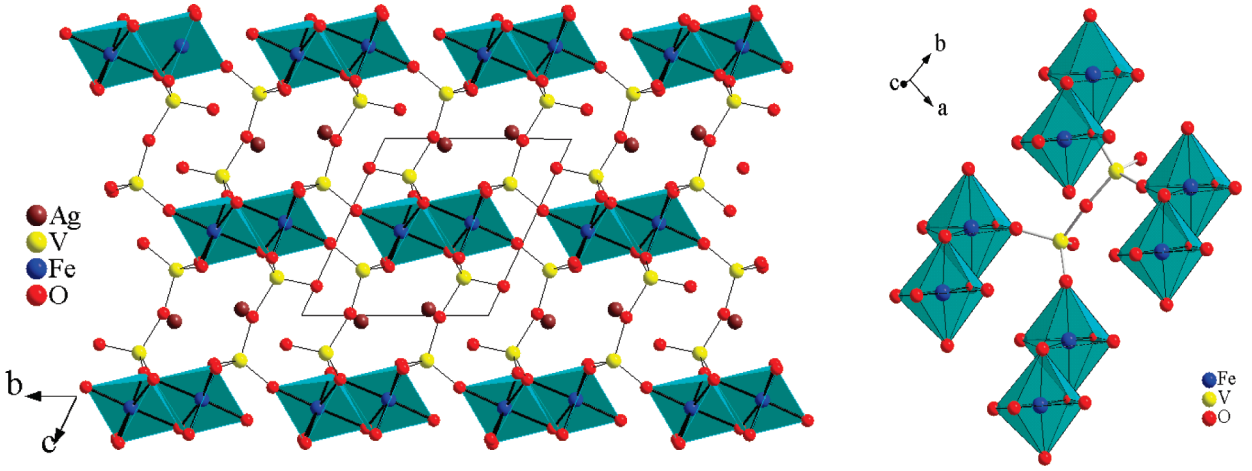

Figure 2. (left) Projected view of the $AgFeV_2O_7$ structure showing $[Fe_2O_{10}]$ dimers interlinked by $[V_2O_7]$ pyrovandates to form channels where Ag^+ reside. (right) Four of the six terminal oxygens of the V_2O_7 unit shared with dimers. The fifth one linking across the *ac* plane, while the sixth oxygen points away from the channel.

to 111.8(2)°, while in $AgFeV_2O_7$, these values are 1.61(3)−1.82(2) Å and 106.0(8)−112.8(7)°, respectively.

Electrochemical Properties. Discharge profiles of the two materials, $Ag_3Fe(VO_4)_2$ and $AgFeV_2O_7$, are shown in Figures 3 and 4, respectively. For $Ag_3Fe(VO_4)_2$, the initial discharge voltage plateau was observed at approximately 3.1 V (Figure 3). After insertion of 0.5 Li, the cell voltage dropped to 2.3 V where a long plateau corresponding to ~2 Li was observed. In total, these two plateaus correspond to the reduction of silver and iron cations. Below 1.7 V, the sloped discharge equates to ca. 1.5 Li's inserted, reflecting reduction of the remaining iron(III) and possibly some vanadium(V) reduction. Overall above 1.5 V, the material reacted with 4 Li's yielding a capacity of 170 mA h/g, close to the expected capacity for the reduction of the silver and iron cations.

Figure 4 shows the discharge profile for $AgFeV_2O_7$, where a long plateau at 2.5 V corresponds to the insertion of one equivalent of lithium, presumably coinciding with reduction of the framework silver. The remaining 3.3 lithiums are inserted on a sloped discharge over an 1.5 V window down to 1.0 V. There appears to be a slope change around 1.7 V, approximately the midpoint. The region between 2.5 and 1.0 V likely corresponds to an overlap of the Fe(III) and V(V) reduction processes. Although layered vanadium oxides are typically reduced between 2 and 2.5 V (vs Li), the tetrahedral coordination of the vanadium(V) cation is known to inhibit the reduction to vanadium(IV), resulting in a lower reduction potential. Nevertheless, the overall capacity is 293 mA h/g. Additional plots for **SFVO-1** (Figure S6) and **SFVO-2** (Figure S7) are given in the Supporting Information.

Discussion

SVO is a layered bronze that contains octahedrally coordinated vanadium oxide layers separated by silver ions in an AgO_n (n = 6) polyhedron. Because of the high coordination number around vanadium (CN > 4), this material exhibits an extended plateau at 2.5 V corresponding to the reduction of the vanadium oxide

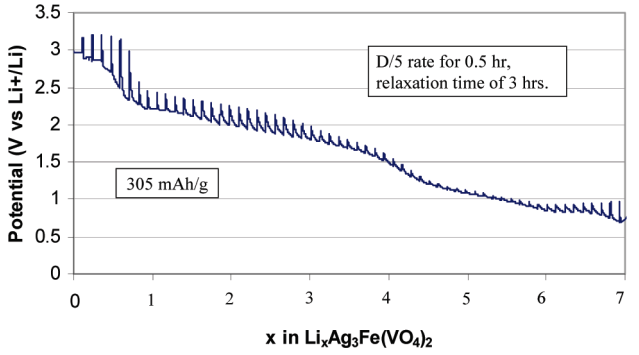

Figure 3. Capacity curve of $Ag_3Fe(VO_4)_2$.

framework (Figure S6).[11] The open nature of the structure combined with good connectivity between the vanadium centers gives this material good electrical conductivity ($\sim 9 \times 10^{-3}$ S/cm) with high power capability. Other materials have been recently reported as candidates for primary lithium batteries, include Ag_2CrO_4, $Ag_4VO_4F_2$, and $AgCuO_2$. However each has yet to surpass SVO at the present time due to various issues ranging from lower energy content and total conductivity to stability in the electrochemical cell environment.

Efforts to increase the power capability in candidate materials for primary lithium batteries have centered on increasing the average discharge voltage. In the case of silver vanadates, an increase in silver content could extend the time the potential is greater than 3 V. Silver pyrovanadate, $Ag_4V_2O_7$, has a Ag:V ratio of 2:1, making it seem like a good candidate. However, its structure is made of $[V_2O_7]^{4-}$ pyrovanadate anions with charge-balancing silver cations arranged in a hexagonally packed net. The electrochemical characterization has not been reported probably because of the molecular nature of the structure which typically yields low intrinsic electronic conductivity and therefore poor performance as a high power cathode material. In addition, the tetrahedral coordination of the vanadium cation makes electrochemical reduction of V^{5+} more difficult, since it is the only formal oxidation state that tetrahedral coordination can accommodate.

Another method to extend the discharge capacity is to "replace" so-called dead weight, tetrahedral V^{5+} in this case, with reducible transition metal cations that have reduction potential window around 2−3 V vs Li/Li^+. Meanwhile, an incentive of choosing iron is based on the fact that the Fe^{3+}/Fe^{2+} reduction potential can reach as high as 3.5 V with a compatible polyanion.[12]

Although materials in the current study have not as of yet had desired overall properties, the new discoveries do offer some features that warrant continued investigation in silver iron(III) vanadate systems for primary lithium-ion battery materials. $Ag_3Fe(VO_4)_2$ has a higher silver/iron to vanadium ration than typical electrochemically

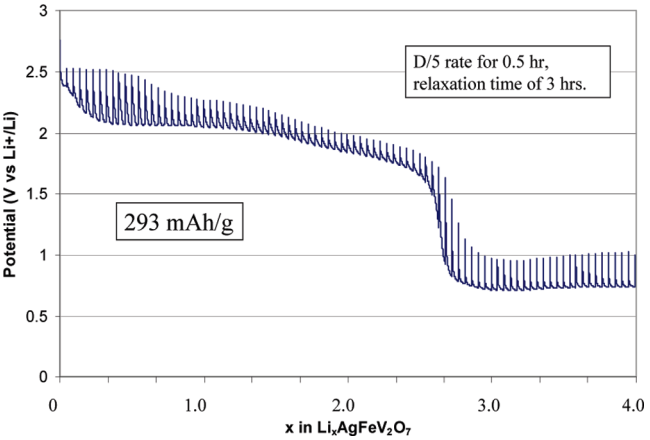

Figure 4. Capacity curve of $AgFeV_2O_7$.

active materials. Layered structures have long been desirable as electrode materials owing to their ability to maintain electrical contacts during lithium insertion and facilitate diffusion within the electrode.[13] In Figure 1, it can be seen that the silver ions lie between sheets of iron oxide octahedra and vanadium oxide tetrahedra. The silver cation position between the iron and vanadium oxide sheets allows for lithium diffusion into the material. $AgFeV_2O_7$ exhibits a channeled structure that is also desirable as electrode materials to maintain their structures under harsh conditions.

The GITT studies were performed on both materials to see the individual reduction potentials and their capacity. $Ag_3Fe(VO_4)_2$ (**SFVO-1**) has two silver reduction events; it is possible to suspect that Ag(2), which has five oxygen atoms in its coordination sphere, has a higher potential than Ag(1), which has four oxygen atoms. The iron's voltage plateau is at 2.25 V, which is in line with other reported iron oxides. To the extent the vanadium cations are reduced, it is observed over a window down to 1.5 V. The vanadium cations have tetrahedral coordination and the V^{5+} tetrahedra cannot be reduced without structural rearrangement to bring more oxide anions to the vanadium coordination sphere. Consequently, the presence of tetrahedral vanadium depresses its reduction potential and modifies the electrochemical behavior of **SFVO-1**.

In $AgFeV_2O_7$ (**SFVO-2**), there is only one silver reduction potential plateau which occurs at 2.5 V. As described earlier, the Ag^+ cations in **SFVO-2** have a distorted square pyramidal geometry; therefore, the one reduction plateau for silver makes sense. The lower than expected voltage could be due to the number of oxygen in its coordination sphere compared to SVO. Also seen in Figure 4, the iron's reduction potential occurs around 2 V, which is again in line with reported iron oxides. In addition, there is a strong covalent interaction between Ag−O(2) via edge-sharing. This pulls Ag away from the other oxygens, making Ag−O(4,6) bonds unusually long. O(4,6), in turn, result in shorter Fe−O(4,6) bonds, which could also lower the

(11) (a) Takeuchi, E. S.; Keister, P. *J. Electrochem. Soc.* **1985**, *132*, C345–C345. (b) Sauvage, F.; Bodenez, V.; Vezin, H.; Morcrette, M.; Mason, T. O.; Tarascon, J.-M.; Poeppelmeier, K. R. *J. Power Sources* **2010**, *195*, 1195–1201.
(12) Salaha, A. A.; Nanjundaswamy, K. S.; Masquelier, C.; Goodenough, J. B. *J. Electrochem. Soc.* **1997**, *144*, 2581–2586.
(13) Whittingham, M. S. *Lithium Ion Batteries, Fundamentals and Performance*; Wakihara, M., Yamamoto, O., Eds.; Wiley-VCH: New York, 1998; pp 49−66.

Fe(III) reduction potential. The vanadium reduction potential is also as expected again taking into account the vanadium's tetrahedral coordination.

However, in both compounds, the capacity is close to or over the theoretical capacity. **SFVO-1** has an initial capacity of 170 mA h/g above 1.5 V equivalent to the insertion of 3.8 mol of lithium per formula unit (Figure 3). It is 95% of the theoretical capacity for the insertion of 4 mol of lithium per formula unit, assuming the vanadium centered tetrahera are electrochemically inactive. **SFVO-2** has a capacity of 293 mA h/g, equaling the insertion of 4 mol of lithium per formula unit, assuming that the V^{5+}/V^{4+} couple is partially active (Figure 4). From the experimental data, the capacity corresponds to 4.3 mol of lithium per formula unit, which suggests that some of the V^{4+} is getting reduced further into V^{3+}. Iron reduction to metal typically occurs well below 1.0 V in related systems. This is due to the channeled structure of the compound, giving greater stability with structural changes.

Final Remarks

Two new silver iron vanadate materials were evaluated as primary batteries in lithium half cells using protocols devised for Ag-containing systems. These new iron(III) containing silver vanadates, $Ag_3Fe(VO_4)_2$ and $AgFeV_2O_7$, are first of the kind that offers extended discharge capacity compared to the commercial cathode material $Ag_2V_4O_{11}$ (SVO). This was achieved by substituting so-called dead weight VO^{3+} isoelectronically with Fe^{3+}. The extended capacity above 2 V (vs Li/Li^+) in these new phases is consistent with their higher $(Ag^+ + Fe^{3+})/V^{5+}$ ratios compared to the corresponding Ag^+/V^{5+} in SVO. However, these compounds suffer the same down fall, where the extended capacity is not all over the 3 V goal. This is likely due to two factors: (1) the vanadate anion having a low inductive effect on the Fe^{3+} cation centers and (2) the Ag^+ cation's coordination being low (CN = 4 and 5). The present studies have shown the proof-of-concept experiments, and we anticipate new materials having an extended capacity due to the addition of the second transition metal (Fe and Mn, for instance) are yet to come. Future studies within the pseudotertiary phase diagram should promise to be very interesting in the primary battery field.

Acknowledgment. Financial support for this research (DMR-0322905, 0706426) and the purchase of a single crystal X-ray diffractometer (CHE-9808165) from the National Science Foundation is gratefully acknowledged.

Supporting Information Available: X-ray crystallographic file (in CIF format) and PXRD, UV−vis diffuse reflectance spectroscopy, OCV, and local structure of Ag^+ cations of **SFVO-1** and **SFVO-2**. This material is available free of charge via the Internet at http://pubs.acs.org.